Full title: PKA and HOG signaling contribute separable roles to anaerobic xylose fermentation in yeast engineered for biofuel production

Short title: PKA and HOG signaling in anaerobic xylose fermentation

Authors: Ellen R. Wagner[1*], Kevin S. Myers[1*], Nicholas M. Riley[2], Joshua J. Coon[2,4,5,6], Audrey P. Gasch[1,3,4]

Affiliations

[1]Great Lakes Bioenergy Research Center, University of Wisconsin – Madison, Madison, WI USA 53706

[2]Department of Chemistry, University of Wisconsin – Madison, Madison, WI USA 53706

[3]Laboratory of Genetics, University of Wisconsin – Madison, Madison, WI USA 53706

[4]Genome Center of Wisconsin, University of Wisconsin – Madison, Madison, WI USA 53706

[5]Department of Biomolecular Chemistry, University of Wisconsin – Madison, Madison WI USA 53706

[6]Morgridge Institute for Research, Madison, WI USA 53715

[*]These authors contributed equally to this work

Corresponding author: agasch@wisc.edu

Abstract

Lignocellulosic biomass offers a sustainable source for biofuel production that does not compete with food-based cropping systems. Importantly, two critical bottlenecks prevent economic adoption: many industrially relevant microorganisms cannot ferment pentose sugars prevalent in lignocellulosic medium, leaving a significant amount of carbon unutilized. Furthermore, chemical biomass pretreatment required to release fermentable sugars generates a variety of toxins, which inhibit microbial growth and metabolism, specifically limiting pentose utilization in engineered strains. Here we dissected genetic determinants of anaerobic xylose fermentation and stress tolerance in chemically pretreated corn stover biomass, called hydrolysate. We previously revealed that loss-of-function mutations in the stress-responsive MAP kinase *HOG1* and negative regulator of the RAS/Protein Kinase A (PKA) pathway, *IRA2*, enhances anaerobic xylose fermentation. However, these mutations likely reduce cells' ability to tolerate the toxins present in lignocellulosic hydrolysate, making the strain especially vulnerable to it. We tested the contributions of Hog1 and PKA signaling via IRA2 or PKA negative regulatory subunit BCY1 to metabolism, growth, and stress tolerance in corn stover hydrolysate and laboratory medium with mixed sugars. We found mutations causing upregulated PKA activity increase growth rate and glucose consumption in various media but do not have a specific impact on xylose fermentation. In contrast, mutation of *HOG1* specifically increased xylose usage. We hypothesized improving stress tolerance would enhance the rate of xylose consumption in hydrolysate. Surprisingly, increasing stress tolerance did not augment xylose fermentation in lignocellulosic medium in this strain background, suggesting other mechanisms besides cellular stress limit this strain's ability for anaerobic xylose fermentation in hydrolysate.

Introduction

Lignocellulosic biomass offers a sustainable source for bioenergy. The use of leftover agriculture byproducts and plants grown on marginal lands for biofuel production reduces waste and removes dependency on food-based cropping systems. Notably, there are two major bottlenecks for sustainable biofuel production from lignocellulosic material. First, many microbes, including industrially relevant *Saccharomyces cerevisiae*, cannot innately ferment pentose sugars like xylose, which comprise a significant fraction of the sugars released from deconstructed biomass (1). Second, the harsh chemical treatment of plant biomass required to release lignocellulosic sugars produces a variety of toxins and stresses that inhibit microbial growth and fermentation (2,3). A goal for the biofuel industry is to engineer stress-tolerant microbes to convert all available sugars to the desired products by routing cellular resources toward product formation and away from cell growth and other unnecessary physiological responses (4).

Several labs have evolved or engineered yeast for anaerobic xylose usage, introducing either xylose isomerase (5–7) or xylose reductase (XR) with xylitol dehydrogenase (XDH) (8–13), and over-expressing xylulokinase for increased flux (14–17). However, most strains do not use xylose unless further evolved through laboratory selection (7,18–21). In some cases, the genetic basis for evolved improvements in anaerobic utilization are known from sequencing of evolved lines. We previously engineered a stress-tolerant strain with XR and XDH (strain Y22-3) and evolved it for aerobic xylose respiration, producing strain Y127. To enable anaerobic xylose fermentation, Y127 was propagated anaerobically on xylose, generating strain Y128 (21). Aerobic xylose respiration in the Y127 strain was enabled by null mutations of the Fe-S cluster protein *ISU1* and the osmotic stress response MAP kinase *HOG1*. Maximal anaerobic fermentation in the evolved Y128 strain was facilitated by these mutations plus additional null mutations of the negative regulator of RAS/PKA signaling, *IRA2*, and *GRE3*, an aldose reductase that siphons xylose to xylitol (22). A subsequent study independently generated an

anaerobic-xylose fermenting strain, confirmed the requirement of the *ISU1* deletion, and further found deletion of the upstream HOG pathway regulator *SSK2* improved xylose fermentation (23). Thus, mutations in these pathways play a generalizable role in anaerobic xylose fermentation across labs and strains.

While mutations that promote xylose utilization are known, the specific roles for each mutation and how the RAS/PKA and HOG pathways intersect to enable anaerobic xylose utilization remain unclear. RAS signaling promotes growth on preferred nutrients like glucose, in part by activating adenylate cyclase to produce cAMP, which binds to the PKA negative regulatory subunit Bcy1 to enable PKA activity (24). Ira1/2 are the GTPase activating proteins (GAPs) that inhibit Ras1/2 by converting GTP (RAS-active state) to GDP (RAS-inactive state). On the other hand, Hog1 is best characterized as an osmotic stress response MAP kinase and leads to the upregulation of stress-responsive transcription factors and other enzymes and defense systems (25). How Hog1 contributes to xylose fermentation is unknown, although the kinase was recently shown to play a role in the response to glucose levels (26–30). PKA and Hog1 have opposing roles on the stress response: PKA activates transcription factors required for growth-promoting genes and directly suppresses stress-activated transcription factors like Msn2/Msn4, while Hog1 activity induces stress-defense regulators and contributes to the repression of growth-promoting genes (31).

Increased stress sensitivity is a major limitation for industrial use of evolved strains with RAS/PKA and HOG mutations and a barrier to sustainable lignocellulosic bioenergy production. Chemical pretreatment of plant biomass is required to release fermentable sugars into the resulting “hydrolysate.” This treatment produces a variety of toxins and stressors that limit microorganisms’ ability to ferment, particularly impacting fermentation and growth during xylose consumption (2,32,33). One group of toxins are lignocellulosic hydrolysate inhibitors (or lignotoxins), which are released from breakdown of hemicellulose and cellulose and include furans, phenolics, and aliphatic acids. Lignotoxins disrupt central carbon metabolism pathways

by generating reactive oxygen species and depleting the cells of ATP, NADH, and NADPH, in part through increased activity of ATP-dependent efflux pumps and detoxification (34–36), ultimately decreasing available resources for growth and metabolism. Therefore, strains must be tolerant to the toxins present in hydrolysate for efficient fermentation of lignocellulosic material, but the mutations required for efficient anaerobic xylose fermentation produce stress-susceptible strains. Upregulated PKA activity suppresses stress-defense pathways (37–40), while *HOG1* deletion decreases cells' ability to mount a stress response. This likely has a direct impact on existing strains, limiting their industrial use. One possible solution is increasing stress tolerance in these strains will enable better anaerobic xylose fermentation in industrially relevant hydrolysates. Other groups have found varying levels of success improving toxin tolerance (3) through overexpression of stress response transcription factors (41,42), mitochondrial NADH-cytochrome b5 reductase (42), an oxidative stress protein kinase (43), and furaldehyde reductases (44), as well as through mating, gene shuffling, and evolution (45–48).

We recently discovered an alternate strategy of enabling anaerobic xylose fermentation, one that we predicted may augment stress tolerance. Perturbing sequence of the PKA regulatory subunit Bcy1 through simple protein fusion (with either a 260 amino acid auxin-inducible degron (AiD) tag without degradation capabilities or merely GFP) promotes anaerobic xylose fermentation equal to strain Y128 without the need for *HOG1* or *IRA2* deletion (93). Since this strain retains functional Hog1 and grows well on glucose, we predicted the strain may have improved stress tolerance, which could enhance growth and xylose fermentation in 9% AFEX-pretreated corn stover hydrolysate (ACSH).

Here, we set out to dissect the contributions of regulators in the RAS/PKA and HOG pathways to anaerobic xylose fermentation, growth, and stress resistance. We demonstrate that while upregulating PKA is important for increased cell growth on glucose, *HOG1* deletion specifically benefits xylose utilization, in part by preventing phosphorylation of glycolytic enzymes by Hog1. Our results show perturbing Bcy1 sequence by protein fusion dramatically

improved stress tolerance, as seen by increased growth in toxic 9% glucan-loading ACSH, but xylose fermentation remained blocked, suggesting physiological stress sensitivity is unlikely the cause of halted xylose consumption in concentrated hydrolysate.

Methods

Strains and Media

Strains used in this study are listed in Table 1. All strains expressed a codon-optimized cassette containing *XYLA* from *Clostridium phytofermentans*, *XYL3* from *Scheffersomyces stipitis*, and *TAL1* from *S. cerevisiae* (21). Generation of strains Y22-3, Y128, Y184, Y184 *ira2Δ*, Y184 *hog1Δ*, Y184 *ira2Δhog1Δ,* Y184 *bcy1Δ*, and 184 Bcy1-AiD was previously described (21,22,93). Y184 *ira2Δbcy1Δ* was made by replacing *BCY1* with *KanMX* marker in Y184 *ira2Δ*, and verified with diagnostic PCRs. *HOG1* was complemented in Y184 *ira2Δhog1Δ* on a low-copy MoBY 1.0 plasmid (49). Site-directed mutagenesis was performed to express the $hog1^{D144A}$ or $hog1^{A844\Delta}$ allele from the MoBY 1.0 plasmid, and correct mutants were verified by sequencing. Strains harboring *HOG1*, $hog1^{D144A}$, or $hog1^{A844\Delta}$ expressing plasmids or the empty-vector control were grown in media containing G418 to maintain the plasmid.

Table 1. Strains used in this study.

Strain ID	Genotype	Reference
Y22-3	NRRL YB-210 MATa spore *HOΔ*	Parreiras et al. 2014
Y128	Y22-3 MATa, $isu1^{C412T}$ $hog1^{A844del}$ $gsh1^{G839A}$ $gre3^{G136A}$ $ira2^{G8782T}$ $sap190^{A2590G}$	Parreiras et al. 2014
Y184	Y22-3 MATa, *isuΔ::loxP-Hyg-loxP, gre3Δ::MR*	Myers et al.,
Y184 *ira2Δ*	Y184, *ira2Δ::MR*	Sato et al., 2016
Y184 *bcy1Δ*	Y184, *bcy1Δ::KanMX*	Myers et al.,
Y184 *hog1Δ*	Y184, *hog1Δ::KanMX*	Sato et al., 2016
Y184 Bcy1-AiD	Y184, BCY1-3' AiD tag (3x Mini-Auxin Induced Degron Sequence-5x FLAG-BCY1-3' UTR-KanMX)	Myers et al.,
Y184 *ira2Δhog1Δ*	Y184, *ira2Δ::MR*, *hog1Δ::KanMX*	Sato et al., 2016
Y184 *ira2Δbcy1Δ*	Y184, ira2*Δ::MR*, *bcy1Δ::KanMX*	This study
Y184 *ira2Δhog1Δ/HOG1*	Y184 *ira2Δhog1Δ*, *HOG1* (CEN4 plasmid: *KanMX*, *URA3*)	This study, Ho et al., 2009
Y184 *ira2Δhog1Δ/*$hog1^{D144A}$	Y184 *ira2Δhog1Δ*, $hog1^{D144A}$ (CEN4 plasmid: *KanMX*, *URA3*)	This study, Ho et al., 2009
Y184 *ira2Δhog1Δ/*$hog1^{A884\Delta}$	Y184 *ira2Δhog1Δ*, $hog1^{A844del}$ (CEN4 plasmid: *KanMX*, *URA3*)	This study, Ho et al., 2009
Y184 *ira2Δhog1Δ/*empty	Y184 *ira2Δhog1Δ*, CEN4 plasmid: *KanMX*, *URA3*	This study, Ho et al., 2009
Y184 *ira2Δ/*empty	Y184 *ira2Δ*, CEN4 plasmid: *KanMX*, *URA3*	This study, Ho et al., 2009

144 YPDX medium was prepared as previously described (50) (1% yeast extract, 2%
145 peptone, except that sugars were added at either 6% glucose and 3% xylose or 9% glucose and
146 4.5% xylose). Identified lignotoxins (51,52) were added to YPDX 6%/3% and the medium was
147 sterilized by vacuum filtration. ACSH was prepared from *Zea mays* (Pioneer hybrid 36H56)
148 grown in Field 570-C Arlington Research Station, University of Wisconsin and harvested in
149 2012, as previously described (53). Pretreated corn stover was hydrolyzed to either 6% or 9%
150 glucan loading at 50°C for 5 days, and biomass was added 4 hours after hydrolysis began in 4
151 batches. The hydrolysate was centrifuged (2500xg for 30 minutes) and sterile filtered (0.22 µm
152 pore size; Millipore Stericup). Final sugar concentrations were 53 g/L glucose and 21.7 g/L
153 xylose for 6% glucan-loading ACSH, and 80 g/L glucose and 36 g/L xylose for 9% glucan-
154 loading ACSH.
155
156 *TECAN Screening*
157 Strains were grown to saturation in YPD 2% batch aerobically overnight, then diluted to
158 an OD_{600} of 2 in YPD 2%. 5 µL of culture was added to 95 µL of 9% ACSH, YPDX 9%/4.5%,
159 YPDX 6%/3%, or YPDX 6%/3% +LT in a Costar clear 96-well plate. OD at 600 nm was
160 measured anaerobically for 48 hours in a TECAN Infinite 200 at 30°C, with measurements taken
161 every 20 minutes (total of 144 measurement cycles) and multiple reads per well. Final OD was
162 calculated based on the average OD reading per well per time point and using three biological
163 replicates. Significant differences compared to Y184 were determined by performing a paired T-
164 test at $p < 0.05$, pairing sample by replicate date.
165
166 *Batch culture fermentations*
167 Overnight aerobic cultures grown in YPD 2% glucose were transferred to an anaerobic
168 chamber, washed once with anaerobic medium, and inoculated into the tested media at an

169 OD_{600} of 0.1. Fermentations occurred for 96 hours, with 1 mL aliquots removed throughout the
170 time course for OD_{600} measurements and HPLC-RID analysis to measure glucose, xylose, and
171 ethanol concentrations. Dry-cell weight biomass was measured by vacuum filtering cultures
172 onto pre-weighed filters (0.45 µm pore size), microwaving on 10% power for 10 minutes, then
173 drying in a desiccant for 24 hours before measuring. Biomass, OD, and concentrations of
174 glucose, xylose, and ethanol were averaged from three biological replicates for each time point.
175 ANOVA was used to determine significant differences in biomass, comparing 24h and 48h
176 within each individual strain, at $p < 0.05$. Rates of sugar consumption were calculated by
177 normalizing the change in sugar concentration to the fitted rate of biomass change during
178 exponential (glucose) or stationary (xylose) phase, and a paired T-test was used to determine
179 significant differences compared to Y184 at $p < 0.05$. Ethanol titer at 48h was averaged from
180 three biological replicates.
181
182 *Phosphoproteomic analysis*
183 Quantitative proteomic and phosphoproteomic samples of Y184 *ira2Δhog1Δ* and Y184
184 *hog1Δ* were prepared as previously described using isobaric tandem mass tags (TMT) for
185 phosphoproteomic analysis (93). Paired samples were collected from two independent
186 replicates grown anaerobically in YPX 3% for three generations and harvested at OD_{600} ~0.5.
187 Proteomic samples were analyzed by nanoflow liquid chromatography tandem mass
188 spectrometry. COMPASS (54) was used to search against target-decoy yeast database (55).
189 Raw data were transformed to $\log_2$ values, then the fold change between Y184 *ira2Δhog1Δ* and
190 Y184 *ira2Δ* peptides was calculated. We focused on differentially abundant phosphopeptides,
191 defined as those with a $\log_2$ difference of at least 1.5X in the same direction in both replicate
192 comparisons. We used this threshold since TMT tagging is known to compress abundance
193 differences (56).

Results

Our goal was to dissect the contributions of different regulators in growth, xylose fermentation, and stress tolerance. We therefore measured fermentation and growth rates of a panel of strains grown in several concentrations of ACSH and laboratory media. To clarify the contribution of each regulator, we started with strain Y22-3, which overexpresses a codon-optimized cassette containing *XYLA* from *Clostridium phytofermentans*, *XYL3* from *Scheffersomyces stipitis*, and *TAL1* from *S. cerevisiae* but cannot utilize xylose, and strain Y184, which additionally lacks *ISU1* and *GRE3* and can thus respire xylose aerobically but not anaerobically (93). Both Y22-3 and Y184 can grow in the toxic 9% ACSH, whereas strain Y128, which can ferment xylose anaerobically, cannot (Fig.1). To test the impact of mutations that enable anaerobic xylose utilization, we generated Y184 derivatives lacking *IRA2*, *BCY1*, or *HOG1* individually as well as *IRA2 HOG1* or *IRA2 BCY1* in combination, to define how each mutation impacts stress tolerance, growth, and metabolism. We also included Y184 Bcy1-AiD, in which an auxin-inducible degradation sequence is fused to the C-terminal of Bcy1 (in the presence of functional *IRA2* and *HOG1*); it is important to note this sequence alone does not enable degradation of Bcy1 but imparts rapid xylose fermentation in lab medium without the need for *HOG1* deletion (93).

Figure 1. Stress susceptibility of strains engineered for xylose consumption. Strains were grown anaerobically in 9% ACSH, YPDX 9%/4.5%, YPDX 6%/3%, and YPDX 6%/3% + lignotoxins (LT) in 96-well plates, and final cell density at 48h was measured with a TECAN instrument. Average and standard deviations of final ODs were calculated from three biological replicates. Asterisks denote significant differences compared to Y184 grown in each respective condition (paired T-Test, $p < 0.05$).

Improving stress tolerance does not restore xylose fermentation in toxic hydrolysate

We first measured tolerance of each strain to ACSH hydrolysates and rich laboratory medium containing mixed glucose/xylose with and without lignotoxins (LT), anaerobically in a 96-well plate reader. 9% ACSH is clearly inhibitory to growth, since all strains grew to much lower cell densities than in rich medium with lignotoxins added (Fig. 1). Parental strains Y22-3 and Y184 showed the best growth in 9% ACSH, as indicated by final cell density, even though they cannot use the xylose after glucose is consumed. Y184 *ira2Δ* and Y184 *bcy1Δ* showed reduced growth compared to Y184, but still grew; Y128, Y184 *hog1Δ*, Y184 *ira2Δhog1Δ*, and Y184 *ira2Δbcy1Δ* were not able to grow. Thus, all strains lacking functional Hog1 showed increased sensitivity to 9% ACSH, as did the Y184 *ira2Δbcy1Δ* strain. Since Hog1 functions in the osmotic stress response, we reasoned the high sugar content of 9% ACSH may be responsible for the sensitivity of *hog1Δ* strains. However, the mutants were not sensitive to rich medium with sugar concentrations matching 9% ACSH (9% glucose, 4.5% xylose, Fig. 1), indicating it is not the osmolarity of 9% ACSH that is inhibitory to these strains. Strikingly, Y184 cells with the Bcy1-AiD tag, which enables anaerobic xylose fermentation, displayed maximal growth in 9% ACSH, comparable to Y184. Therefore, as we predicted, Y184 Bcy1-AiD lacks the extreme stress sensitivity seen in *hog1Δ* strains. While adding lignotoxins to YPDX medium decreased growth, it was not as inhibitory to any strain as 9% ACSH, suggesting either the lignotoxin cocktail (52) added was lower than toxin levels in real hydrolysate or additional toxins not in our cocktail remain to be identified.

We next studied glucose and xylose consumption in 9% ACSH to characterize fermentation rates. We expected the strains whose growth was sensitive to the stresses of ACSH would ferment worse compared to tolerant strains. Surprisingly, we found all strains, even those containing functional Hog1, were incapable of fermenting xylose in hydrolysate

244 generated at high-glucan loading (Fig. 2C, Fig. S1C). Y128 and Y184 *hog1Δ* did not grow to
245 densities as high as Y184, but Y184 Bcy1-AiD showed division as robust as Y184 (Fig. 2A),
246 supporting observations seen with the 96-well plate screen. Consistent with our hypothesis,
247 Y184 *hog1Δ* and especially Y128 cultures showed reduced glucose consumption over the time
248 course, whereas stress-tolerant Y184 and Y184 Bcy1-AiD depleted the glucose by 40 hours
249 (Fig. 2B). Since we previously showed the Y184 Bcy1-AiD strain can ferment xylose
250 anaerobically at higher rates than Y128 in laboratory medium (93) and has dramatically
251 improved growth in 9% ACSH, we predicted Y184 Bcy1-AiD would display enhanced xylose
252 consumption compared to Y128 and Y184 *hog1Δ* in 9% ACSH. Unexpectedly, this was not
253 observed, as none of the strains used xylose in 9% ACSH (Fig. 2C) even though two fermented
254 the glucose. Several strains marginally used xylose in 6% ACSH (Fig. S2C), but clearly ferment
255 xylose in YPDX (see below), this suggests stresses in ACSH medium prevent xylose
256 fermentation. Since the growth and glucose consumption of Y184 Bcy1-AiD is clearly recovered,
257 these results suggest cellular stress is unlikely to be the cause of arrested xylose fermentation
258 (see Discussion).
259
260 **Figure 2. 9% ACSH is inhibitory to xylose fermentation.** Batch cultures of Y128, Y184, Y184
261 *hog1Δ*, and Y184 Bcy1-AiD were grown anaerobically for 92 hours in 9% ACSH. **A.** Average
262 OD_{600} measurements from three biological replicates over time for denoted strains. **B.** Glucose
263 concentration over time for strains grown in (A). **C.** Xylose concentration over time for the same
264 cultures shown in (A).
265
266 *Differential contributions of regulators to glucose versus xylose fermentation rates*
267 We next wanted to dissect the contribution of Ira2, Bcy1, and Hog1 to sugar
268 fermentation. We worked with laboratory media supplemented with 60 g/L glucose and 30 g/L

xylose to characterize fermentation when the strains are most productive, since they did not ferment xylose efficiently in ACSH. Interestingly, strains lacking Ira2 or Bcy1 or harboring the Bcy1-AiD fusion protein showed faster growth compared to the parental strains: all strains with these mutations reached maximum cell density by 24h, whereas Y22-3, Y184, and Y184 *hog1Δ* took 48h to reach maximal titers (Fig. 3A, Fig. S3A). Although it was not statistically significant in this growth assay, we noticed in the 96-well plate assay (Fig. 1) strains lacking *IRA2* or *BCY1* consistently grew to lower cell densities than the parental strains. Deletion of *HOG1* from Y184 reduced growth rate and glucose consumption rate compared to the other strains, whereas combined deletions of *HOG1* and *IRA2* produced a strain with fast growth rates and the ability to grow to a higher cell density than Y22-3 and Y184 (Fig. 3A,B, Fig. S3A,B). Thus, the beneficial effect of *IRA2* deletion overrides the deleterious effect of *HOG1* deletion for glucose-based growth.

Figure 3. PKA activity increases growth, while *hog1Δ* improves xylose consumption. Batch cultures were grown in YPDX 6%/3% for 96 hours. Measurements are averages from three biological replicates. **A.** The average dry-cell weight biomass (g per L culture) measured at 6, 24, and 48 h post inoculation. Asterisk indicates a significant difference ($p < 0.055$) between the 24h and 48h timepoint within each strain. For all strains except Y184 and Y184 *hog1Δ*, the biomass accumulated was not significantly different at 48h compared to 24h, indicating faster saturation of those cultures. **B.** Specific glucose consumption rates calculated from the exponential phase of growth. **C.** Specific xylose consumption rate calculated from the stationary phase of growth. **D.** Ethanol titer at 48 hours post inoculation. For **B,C,D**, asterisks denote significant differences compared to Y184 (paired T-Test, $p < 0.05$).

While mutations in PKA regulators increase growth on and consumption of glucose, the opposite was observed for xylose consumption. Strains lacking *HOG1* had the highest rates of xylose consumption compared to the parental strains, whereas strains with PKA mutations alone did not have a significantly different xylose consumption rate from the Y184 parental strain (Fig. 3C). Thus, mutating *HOG1* is specifically important for efficient xylose fermentation. Moreover, Y128, Y184 *hog1Δ*, and Y184 *ira2Δhog1Δ* begin to ferment the xylose before glucose is completely depleted from the culture (Fig. S3B and C). Correspondingly, Y128, Y184 *hog1Δ*, and Y184 *ira2Δhog1Δ* had the highest ethanol titer at 48 hours (Fig. 3D, Fig. S3D). Y184 Bcy1-AiD was previously shown to use xylose at a comparable rate to Y128 in YPX medium when cultured at a high cell density (93). Interestingly, we discovered that the strain does not use xylose efficiently when the culture is started at low cell density (Fig. 3C), even though we recapitulate robust xylose utilization at high cell density in YPDX (Fig. S4A). The reason for this unique phenotype is not known; importantly, it did not explain the lack of xylose consumption in ACSH, since inoculating cultures at high cell titers did not improve xylose fermentation in the strain (Fig. S4B).

Hog1 kinase activity decreases xylose fermentation

HOG1 deletion allows for efficient xylose fermentation in YPDX. To test if it is the kinase activity of Hog1, as opposed to other effects of the Hog1 protein, we tested if the catalytically inactive *hog1-D144A* allele or truncated *HOG1* recapitulating Y128's mutation (*hog1 A844Δ*) could block xylose fermentation when introduced into Y184 *ira2Δhog1Δ*, equal to reintroducing the functional *HOG1* allele. We saw the catalytic activity of Hog1 was required to suppress anaerobic xylose fermentation: reintroducing wildtype *HOG1* increased glucose consumption and inhibited xylose fermentation, whereas expression of catalytically inactive or truncated Hog1 did not significantly affect the glucose or xylose consumption rate, since the strains matched the

318 performance of Y184 *ira2Δhog1Δ* (Fig. 4). This reveals Hog1 kinase activity normally inhibits
319 xylose fermentation, suggesting Hog1 actively phosphorylates one or more targets to prevent
320 xylose utilization.
321
322 **Figure 4. Hog1 activity blocks xylose consumption.** Wildtype, catalytically inactive
323 (*hog1*^{D144A}), and truncated (*hog1*$^{A844\Delta}$) *HOG1* alleles were expressed in Y184 *ira2Δhog1Δ* cells
324 and grown in batch culture for 96 hours in YPDX 6%/3%. Rate measurements were based on
325 average and standard deviation from three biological replicates. **A.** Average growth rate
326 calculated from the exponential phase of growth. **B.** Specific glucose consumption rate
327 calculated from the exponential phase of growth. **C.** Specific xylose consumption rate calculated
328 from the stationary phase of growth. Asterisks denote significant differences from Y184
329 *ira2Δhog1Δ*/*HOG1* (paired T-Test, $p < 0.05$).
330
331 We performed phosphoproteomic analysis to implicate potential Hog1 targets impacting
332 xylose consumption. Y184 *ira2Δ* and Y184 *ira2Δhog1Δ* were grown anaerobically in batch
333 culture in YPX medium, and phospho-proteomes were measured by quantitative mass-
334 spectrometry (see Methods). We identified only 11 phosphopeptides whose abundance was
335 reproducibly lower in Y184 *ira2Δhog1Δ* (Table 2, see methods). Of these 11, four are linked to
336 metabolism: E1 alpha subunit of pyruvate dehydrogenase (Pda1), pyruvate kinase (Cdc19),
337 glyceraldehyde-3-phosphate dehydrogenase (Tdh1), and trehalose-6-phosphatase complex
338 (Tsl1). Pda1, Cdc19, and Tdh1 have roles in glycolysis, whereas Tsl1 generates the overflow
339 metabolite trehalose. In contrast, eight phosphopeptides showed reproducibly increased
340 abundance in Y184 *ira2Δhog1Δ*. Of these eight, four are from proteins with unknown functions,
341 one is a heat shock protein (Hsp26), two are components of the 40S ribosome (Rps6A, Rps6B),
342 and one is an epsin-like protein involved in endocytosis (Table 2). Several of these enzymes,

including Cdc19 and Tsl1, directly interact with Hog1, and others harbor the known Hog1 consensus sites around the affected residue, suggesting Hog1 directly phosphorylates these proteins (see Discussion).

Table 2. Peptides with phosphorylation changes in Y184 *ira2Δhog1Δ*

Protein	Common Name	Phospho Site	Direction of change in Y184 *ira2 Δhog1 Δ*
YJL136C	RPS21B	S65	Decreased
YER178W	PDA1	S336	Decreased
YER178W	PDA1	S344	Decreased
YDL223C	HBT1	S41	Decreased
YMR031C	EIS1	S736	Decreased
YAL038W	CDC19	S22	Decreased
YMR031C	EIS1	T767	Decreased
YDL223C	HBT1	S363	Decreased
YJL052W	TDH1	T136	Decreased
YPL118W	MRP51	S327	Decreased
YML100W	TSL1	S266	Decreased
YBR072W	HSP26	S208	Increased
YNL115C	YNL115C	S244	Increased
YNL115C	YNL115C	S42	Increased
YDL161W	ENT1	S317	Increased
YBR181C	RPS6B	S232	Increased
YPL090C	RPS6A	S232	Increased
YLR413W	INA1	S654; S657	Increased
YLR413W	INA1	S652; S657	Increased

Discussion

Our results provide new insights into how mutation of different signaling proteins can impart distinct physiological responses that, when integrated, improve anaerobic conversion of sugars to products, in this case ethanol. We show mutations in RAS/PKA signaling that up-regulate PKA activity enhance growth and perhaps glucose consumption rates, but possibly at a cost of final cell density, whereas deletion of HOG1 is essential for xylose fermentation but at the expense of hydrolysate tolerance. Together, these results suggest several important results relevant to lignocellulosic fermentation.

PKA and Hog1 contribute separable features to xylose fermentation. Increased PKA activity is known to increase cell growth rate and glucose consumption (57). PKA upregulates

359 expression of ribosome biogenesis genes, which supports rapid growth (58,59). Moreover, it
360 promotes glycolytic flux by inducing transcription of genes and phosphorylating enzymes
361 involved in glycolysis (60–62). We recently showed PKA also has roles in the hypoxic response
362 when cells are grown anaerobically on xylose (93). This response is mediated by the Azf1 and
363 Mga2 transcription factors and may further promote glycolytic flux. Therefore, it is consistent
364 that we find strains with deletions of RAS/PKA regulators display faster growth (Fig. 3A, Fig.
365 S3A). Despite the increased growth and glucose consumption rates when PKA regulators are
366 deleted, this effect is not as dramatic with xylose. While strains with mutations in *IRA2* or *BCY1*
367 do consume more xylose than Y184 (Fig. S3C), the rates of consumption are not significantly
368 faster than Y184 (Fig. 3C). The reduced final-cell titers seen in strains with up-regulated
369 RAS/PKA may result from an inability to accumulate storage carbohydrates. During the diauxic
370 shift, glycogen storage occurs when glucose has been depleted to fifty percent of its starting
371 concentration (63). However, increased PKA activity prevents accumulation of storage
372 carbohydrates, such as glycogen and trehalose, by inhibiting expression of biosynthesis
373 enzymes and activating catabolic enzymes (64–68). In our strains lacking RAS/PKA inhibitors, it
374 is possible upon glucose depletion, the cells lack stored carbohydrates to metabolize, limiting
375 cell titers compared to strains with functional *IRA2* and *BCY1* (Fig. 1, Fig. S3A).
376 In contrast to PKA upregulation, *HOG1* deletion specifically affects xylose utilization. Our
377 results show that under standard conditions, even in the absence of added stress, Hog1 kinase
378 activity inhibits xylose utilization, perhaps by directly phosphorylating glycolytic enzymes (Fig.
379 4C, Table 2). Although typically thought of as a stress regulator, Hog1 has recently been
380 implicated in the response to glucose (28,29,69) and was shown to phosphorylate the glycolytic
381 enzyme Pfk26 (70) and physically interact with Cdc19, Pfk1, and Pfk2 (71). Hog1 also plays an
382 important role in glycerol production, which may influence glycolytic flux to steer production from
383 pyruvate towards glycerol (72–77). The enzymes we detected with significant phosphorylation
384 differences upon *HOG1* deletion function lower in glycolysis, after the entry point of xylose via

385 the pentose phosphate pathway (Table 2), but we cannot exclude that other enzymes or
386 regulators are also affected. Modeling of glycolytic flux during osmoadaption suggests Hog1
387 activity stabilizes pyruvate production to prevent starvation (75), which may account for the
388 decreased phosphorylation of Cdc19's activation site in *hog1Δ* mutants (Table 2).
389
390 An interesting question is the relationship between PKA and Hog1 activity. We
391 previously found Y184 *bcy1Δ* cells display reduced phosphorylation of the Hog1 protein on its
392 activating site when grown anaerobically in YPX medium (93), suggesting a PKA-dependent
393 mechanism of inhibiting Hog1 activity to allow xylose fermentation. Hog1 was shown to be
394 activated during glucose depletion (28,69). It is possible as cells begin to deplete glucose from
395 YPDX, Hog1 becomes activated in Y184 but that this is suppressed when PKA is up-regulated
396 via *BCY1* or *IRA2* deletion. The largest effects on xylose metabolism occur when PKA
397 upregulation and *HOG1* deletion are combined. Unfortunately, a byproduct of this is likely
398 causing extreme stress sensitivity. Strains lacking *HOG1* (Y128, Y184 *hog1Δ*, and Y184
399 *ira2Δhog1Δ*) are especially sensitive to hydrolysate (Fig. 1, Fig. 2A, Fig. S1A). Moreover, the
400 combination of upregulated PKA and *HOG1* deletion may exacerbate stress sensitivity, since
401 PKA suppresses the stress response (24), while Hog1 activates it (25). These strains are able
402 to ferment xylose in favorable conditions (Fig. 3C, Fig. S3C), but are unable to ferment the
403 sugar in toxic 9% ACSH (Fig. 2C, Fig. S1C).
404 We hypothesized improving stress tolerance would improve xylose fermentation in
405 stressful conditions. We predicted Y184 Bcy1-AiD, which harbors functional *HOG1* but can
406 ferment xylose anaerobically in rich medium when started at high titers (93), would display both
407 higher stress tolerance and anaerobic xylose fermentation in hydrolysate. Interestingly, while
408 Y184 Bcy1-AiD clearly grew well in 9% ACSH, it did not utilize the xylose even when started at
409 high cell titer (Fig. 1, Fig. 2A, Fig. 2C Fig. S4B). This suggests stress sensitivity is not the sole

410 factor limiting xylose fermentation. There are many types of lignotoxins present in hydrolysates
411 (51), and while their effects are somewhat understood, many of their specific targets remain to
412 be elucidated (33). One possibility is that toxins are directly inhibiting enzymes required for
413 anaerobic xylose fermentation, as shown in *Escherichia coli* where feruloyl and coumaroyl
414 amides were discovered to be allosteric inhibitors of *de novo* nucleotide biosynthetic enzymes
415 (78). Jayakody et al. (2018) found that glycoaldehyde and methyglyoxal present in hydrolysate
416 are key inhibitors of xylose fermentation (79). Furthermore, acetic acid is known to decrease
417 enolase activity, ultimately slowing down glycolysis (80). This has led to other groups
418 engineering yeast to reduce and ferment acetate or increase acetate tolerance (43,81,82). More
419 studies identifying the targets of lignotoxins will help to clarify the bottleneck in xylose
420 metabolism when microorganisms are grown in hydrolysate media.

421 Our results also revealed unexpected information on the different routes of PKA
422 regulation with regard to the stress response. Removing either *IRA2* or *BCY1* had mild impacts
423 on ACSH tolerance, but deletion of both genes greatly impacted tolerance of 9% ACSH (Fig. 1,
424 Fig. 2A, Fig. S1A). This suggests there are multiple lines of partially redundant regulation of
425 stress tolerance by the RAS/PKA pathways. Upregulation RAS by *IRA2* deletion is predicted to
426 increase cAMP and thus PKA activity (83), whereas deletion of *BCY1* removes the cAMP-
427 responsive inhibitor of PKA. One possibility is PKA is only partially upregulated by single-gene
428 deletion, but double-deletion of *IRA2* and *BCY1* produces much stronger activation and thus
429 complete suppression of the stress response. There are other methods of RAS/PKA pathway
430 regulation which support the possibility that single deletion of *IRA2* or *BCY1* causes only a
431 partial upregulation. The RAS/PKA pathway undergoes feedback inhibition to control cAMP
432 concentrations through predicted PKA-directed phosphorylation of Cdc25 and Pde1 (84).
433 Furthermore, the interaction between the catalytic and regulatory subunits of PKA is regulated
434 by other factors, including kelch-repeat proteins Krh1/2 (85). Another possibility is PKA may be
435 directed to different substrates in different situations. Beyond allosteric cAMP regulation

436 influenced by RAS, Bcy1 is also regulated by phosphorylation, which can influence PKA
437 substrate specificity and localization (86–90). Recent studies in mammalian cells show the
438 negative regulator of PKA does not dissociate from the active kinase at physiological cAMP
439 levels (91), and the substrate determines the dissociation rate of catalytic and regulatory
440 subunits (92). Thus, activation of PKA via Bcy1-cAMP binding may provide different effects than
441 if Bcy1 is missing from the cell. Finally, it is also possible that PKA-independent effects of *IRA2*
442 deletion separately regulate the stress response. Future studies to dissect these and other
443 effects will contribute to our understanding of how to engineer cells for anaerobic xylose
444 fermentation in lignocellulosic hydrolysates.
445

446 **Acknowledgments**

447 We thank Trey Sato for providing strains, Mick McGee for HPLC analysis, and members of the
448 Gasch lab for constructive discussions.
449

450 **Author Contributions**

451 Conceptualization: ERW, KSM, and APG. Investigation: ERW, KSM, and NMR. Methodology:
452 ERW, KSM, NMR, JJC, and APG. Formal Analysis: ERW, KSM, and APG. Funding Acquisition:
453 APG and JJC. Project Administration: APG. Resources: APG and JJC. Software: KSM, NMR,
454 JJC, and APG. Supervision: APG. Validation. ERW, KSM, and APG. Visualization: ERW, KSM,
455 and APG. Writing- Original Draft Preparation: ERW and APG. Writing – Review & Editing: ERW,
456 KSM, and APG.
457

458 **References**

459 1. van Maris AJA, Abbott DA, Bellissimi E, van den Brink J, Kuyper M, Luttik MAH, et al.
460 Alcoholic fermentation of carbon sources in biomass hydrolysates by *Saccharomyces*

cerevisiae: current status. Antonie Van Leeuwenhoek. 2006 Nov 11;90(4):391–418.

2. Klinke HB, Thomsen AB, Ahring BK. Inhibition of ethanol-producing yeast and bacteria by degradation products produced during pre-treatment of biomass. Appl Microbiol Biotechnol. 2004 Nov 6;66(1):10–26.

3. Caspeta L, Castillo T, Nielsen J. Modifying yeast tolerance to inhibitory conditions of ethanol production processes. Front Bioeng Biotechnol. 2015 Nov 11;3:184.

4. Deparis Q, Claes A, Foulquié-Moreno MR, Thevelein JM. Engineering tolerance to industrially relevant stress factors in yeast cell factories. FEMS Yeast Res. 2017 Jun 1;17(4): doi:10.1093/femsyr/fox036.

5. Kuyper M, Harhangi H, Stave A, Winkler A, Jetten M, Delaat W, et al. High-level functional expression of a fungal xylose isomerase: the key to efficient ethanolic fermentation of xylose by ? FEMS Yeast Res. 2003 Oct 1;4(1):69–78.

6. Kuyper M, Hartog M, Toirkens M, Almering M, Winkler A, Vandijken J, et al. Metabolic engineering of a xylose-isomerase-expressing strain for rapid anaerobic xylose fermentation. FEMS Yeast Res. 2005 Feb 1;5(4–5):399–409.

7. Demeke MM, Dietz H, Li Y, Foulquié-Moreno MR, Mutturi S, Deprez S, et al. Development of a D-xylose fermenting and inhibitor tolerant industrial *Saccharomyces cerevisiae* strain with high performance in lignocellulose hydrolysates using metabolic and evolutionary engineering. Biotechnol Biofuels. 2013 Jun 21;6(1):89.

8. Ho NW, Chen Z, Brainard AP. Genetically engineered *Saccharomyces* yeast capable of effective cofermentation of glucose and xylose. Appl Environ Microbiol. 1998 May 1;64(5):1852–9.

9. Jin Y-S, Seo H. Conversion of xylose to ethanol by recombinant *Saccharomyces cerevisiae* containing genes for xylose reductase and xylitol dehydrogenase from *Pichia stipitis*. J Microbiol Biotechnol. 2000;10(4): 564-567.

10. Kötter P, Amore R, Hollenberg CP, Ciriacy M. Isolation and characterization of the *Pichia*

stipitis xylitol dehydrogenase gene, *XYL2*, and construction of a xylose-utilizing *Saccharomyces cerevisiae* transformant. Curr Genet. 1990;18(6):493–500.

11. Walfridsson M, Hallborn J, Penttilä M, Keränen S, Hahn-Hägerdal B. Xylose-metabolizing *Saccharomyces cerevisiae* strains overexpressing the *TKL1* and *TAL1* genes encoding the pentose phosphate pathway enzymes transketolase and transaldolase. Appl Environ Microbiol. 1995 Dec 1;61(12):4184–90.

12. Jin Y-S, Jeffries TW. Changing flux of xylose metabolites by altering expression of xylose reductase and xylitol dehydrogenase in recombinant *Saccharomyces cerevisiae*. In: Davison BH, Lee JW, Finkelstein M, McMillan JD, editors. Biotechnology for Fuels and Chemicals. Totowa, NJ: Humana Press; 2003. pp. 277–85.

13. Kim SR, Ha S-J, Kong II, Jin Y-S. High expression of *XYL2* coding for xylitol dehydrogenase is necessary for efficient xylose fermentation by engineered *Saccharomyces cerevisiae*. Metab Eng. 2012 Jul 1;14(4):336–43.

14. Johansson B, Christensson C, Hobley T, Hahn-Hägerdal B. Xylulokinase overexpression in two strains of *Saccharomyces cerevisiae* also expressing xylose reductase and xylitol dehydrogenase and its effect on fermentation of xylose and lignocellulosic hydrolysate. Appl Environ Microbiol. 2001 Sep 1;67(9):4249–55.

15. Toivari MH, Aristidou A, Ruohonen L, Penttilä M. Conversion of xylose to ethanol by recombinant *Saccharomyces cerevisiae*: importance of xylulokinase (*XKS1*) and oxygen availability. Metab Eng. 2001 Jul 1;3(3):236–49.

16. Jin Y-S, Jones S, Shi N-Q, Jeffries TW. Molecular cloning of *XYL3* (D-xylulokinase) from *Pichia stipitis* and characterization of its physiological function. Appl Environ Microbiol. 2002 Mar 1;68(3):1232–9.

17. Jin Y-S, Ni H, Laplaza JM, Jeffries TW. Optimal growth and ethanol production from xylose by recombinant *Saccharomyces cerevisiae* require moderate D-xylulokinase activity. Appl Environ Microbiol. 2003 Jan 1;69(1):495–503.

513 18. Kim SR, Ha S-J, Wei N, Oh EJ, Jin Y-S. Simultaneous co-fermentation of mixed sugars:
514 a promising strategy for producing cellulosic ethanol. Trends Biotechnol. 2012 May
515 1;30(5):274–82.
516 19. Kim SR, Skerker JM, Kang W, Lesmana A, Wei N, Arkin AP, et al. Rational and
517 evolutionary engineering approaches uncover a small set of genetic changes efficient for
518 rapid xylose fermentation in *Saccharomyces cerevisiae*. PLoS One. 2013 Feb 26;8(2):
519 doi:10.1371/journal.pone.0057048.
520 20. Diao L, Liu Y, Qian F, Yang J, Jiang Y, Yang S. Construction of fast xylose-fermenting
521 yeast based on industrial ethanol-producing diploid *Saccharomyces cerevisiae* by rational
522 design and adaptive evolution. BMC Biotechnol. 2013 Dec 19;13(1): doi:10.1186/1472-
523 6750-13-110.
524 21. Parreiras LS, Breuer RJ, Avanasi Narasimhan R, Higbee AJ, La Reau A, Tremaine M, et
525 al. Engineering and two-stage evolution of a lignocellulosic hydrolysate-tolerant
526 *Saccharomyces cerevisiae* strain for anaerobic fermentation of xylose from AFEX
527 pretreated corn stover. PLoS One. 2014 Sep 15;9(9): doi:10.1371/journal.pone.0107499.
528 22. Sato TK, Tremaine M, Parreiras LS, Hebert AS, Myers KS, Higbee AJ, et al. Directed
529 evolution reveals unexpected epistatic interactions that alter metabolic regulation and
530 enable anaerobic xylose use by *Saccharomyces cerevisiae*. PLOS Genet. 2016 Oct
531 14;12(10): doi:10.1371/journal.pgen.1006372.
532 23. dos Santos LV, Carazzolle MF, Nagamatsu ST, Sampaio NMV, Almeida LD, Pirolla RAS,
533 et al. Unraveling the genetic basis of xylose consumption in engineered *Saccharomyces*
534 *cerevisiae* strains. Sci Rep. 2016 Dec 21;6(1): doi.org/10.1038/srep38676.
535 24. Conrad M, Schothorst J, Kankipati HN, Van Zeebroeck G, Rubio-Texeira M, Thevelein
536 JM. Nutrient sensing and signaling in the yeast *Saccharomyces cerevisiae*. FEMS
537 Microbiol Rev. 2014 Mar 1;38(2):254–99.
538 25. Saito H, Posas F, Horecka J, DePinho RA, Sprague GF, Tyers M, et al. Response to

539 hyperosmotic stress. Genetics. 2012 Oct 1;192(2):289–318.

540 26. Remize F, Cambon B, Barnavon L, Dequin S. Glycerol formation during wine
541 fermentation is mainly linked to Gpd1p and is only partially controlled by the HOG
542 pathway. Yeast. 2003 Nov 1;20(15):1243–53.

543 27. Jiménez-Martí E, Zuzuarregui A, Gomar-Alba M, Gutiérrez D, Gil C, del Olmo M.
544 Molecular response of *Saccharomyces cerevisiae* wine and laboratory strains to high
545 sugar stress conditions. Int J Food Microbiol. 2011 Jan 31;145(1):211–20.

546 28. Piao H, MacLean Freed J, Mayinger P. Metabolic activation of the HOG MAP kinase
547 pathway by Snf1/AMPK regulates lipid signaling at the Golgi. Traffic. 2012 Nov
548 1;13(11):1522–31.

549 29. Tomás-Cobos L, Casadomé L, Mas G, Sanz P, Posas F. Expression of the HXT1 low
550 affinity glucose transporter requires the coordinated activities of the HOG and glucose
551 signalling pathways. J Biol Chem. 2004 May 21;279(21):22010–9.

552 30. Gomar-Alba M, Morcillo-Parra MÁ, Olmo M del. Response of yeast cells to high glucose
553 involves molecular and physiological differences when compared to other osmostress
554 conditions. FEMS Yeast Res. 2015 Aug 1;15(5): doi:10.1093/femsyr/fov039.

555 31. Ho Y-H, Gasch AP. Exploiting the yeast stress-activated signaling network to inform on
556 stress biology and disease signaling. Curr Genet. 2015 Nov 10;61(4):503–11.

557 32. Ask M, Bettiga M, Duraiswamy V, Olsson L. Pulsed addition of HMF and furfural to batch-
558 grown xylose-utilizing *Saccharomyces cerevisiae* results in different physiological
559 responses in glucose and xylose consumption phase. Biotechnol Biofuels. 2013 Dec
560 16;6(1): doi:10.1186/1754-6834-6-181.

561 33. Piotrowski JS, Zhang Y, Bates DM, Keating DH, Sato TK, Ong IM, et al. Death by a
562 thousand cuts: the challenges and diverse landscape of lignocellulosic hydrolysate
563 inhibitors. Front Microbiol. 2014 Mar 14;5: doi:10.3389/fmicb.2014.00090

564 34. Almeida JRM, Runquist D, Sànchez Nogué V, Lidén G, Gorwa-Grauslund MF. Stress-

related challenges in pentose fermentation to ethanol by the yeast *Saccharomyces cerevisiae*. Biotechnol J. 2011 Mar 1;6(3):286–99.

35. Modig T, Lidén G, Taherzadeh MJ. Inhibition effects of furfural on alcohol dehydrogenase, aldehyde dehydrogenase and pyruvate dehydrogenase. Biochem J. 2002 May 1;363(Pt 3):769–76.

36. Heer D, Sauer U. Identification of furfural as a key toxin in lignocellulosic hydrolysates and evolution of a tolerant yeast strain. Microb Biotechnol. 2008 Nov 1;1(6):497–506.

37. Marchler G, Schüller C, Adam G, Ruis H. A *Saccharomyces cerevisiae* UAS element controlled by protein kinase A activates transcription in response to a variety of stress conditions. EMBO J. 1993 May 1;12(5):1997–2003.

38. Stanhill A, Schick N, Engelberg D. The yeast ras/cyclic AMP pathway induces invasive growth by suppressing the cellular stress response. Mol Cell Biol. 1999 Nov 1;19(11):7529–38.

39. Trott A, Shaner L, Morano KA. The molecular chaperone Sse1 and the growth control protein kinase Sch9 collaborate to regulate protein kinase A activity in *Saccharomyces cerevisiae*. Genetics. 2005 Jul;170(3):1009–21.

40. Park J-I, Collinson EJ, Grant CM, Dawes IW. Rom2p, the Rho1 GTP/GDP exchange factor of *Saccharomyces cerevisiae*, can mediate stress responses via the Ras-cAMP pathway. J Biol Chem. 2005 Jan 28;280(4):2529–35.

41. Sasano Y, Watanabe D, Ukibe K, Inai T, Ohtsu I, Shimoi H, et al. Overexpression of the yeast transcription activator Msn2 confers furfural resistance and increases the initial fermentation rate in ethanol production. J Biosci Bioeng. 2012 Apr 1;113(4):451–5.

42. Wallace-Salinas V, Signori L, Li Y-Y, Ask M, Bettiga M, Porro D, et al. Re-assessment of *YAP1* and *MCR1* contributions to inhibitor tolerance in robust engineered *Saccharomyces cerevisiae* fermenting undetoxified lignocellulosic hydrolysate. AMB Express. 2014 Dec 22;4(1): doi:10.1186/s13568-014-0056-5.

591 43. Oh EJ, Wei N, Kwak S, Kim H, Jin Y-S. Overexpression of *RCK1* improves acetic acid
592 tolerance in *Saccharomyces cerevisiae*. J Biotechnol. 2019 Feb 20;292:1–4.
593 44. Almeida JRM, Bertilsson M, Hahn-Hägerdal B, Lidén G, Gorwa-Grauslund M-F. Carbon
594 fluxes of xylose-consuming *Saccharomyces cerevisiae* strains are affected differently by
595 NADH and NADPH usage in HMF reduction. Appl Microbiol Biotechnol. 2009 Sep
596 9;84(4):751–61.
597 45. Zheng D-Q, Wu X-C, Tao X-L, Wang P-M, Li P, Chi X-Q, et al. Screening and
598 construction of *Saccharomyces cerevisiae* strains with improved multi-tolerance and
599 bioethanol fermentation performance. Bioresour Technol. 2011 Feb 1;102(3):3020–7.
600 46. Demeke MM, Dumortier F, Li Y, Broeckx T, Foulquié-Moreno MR, Thevelein JM.
601 Combining inhibitor tolerance and D-xylose fermentation in industrial *Saccharomyces*
602 *cerevisiae* for efficient lignocellulose-based bioethanol production. Biotechnol Biofuels.
603 2013 Aug 26;6(1): doi:10.1186/1754-6834-6-120.
604 47. Smith J, van Rensburg E, Görgens JF. Simultaneously improving xylose fermentation
605 and tolerance to lignocellulosic inhibitors through evolutionary engineering of recombinant
606 *Saccharomyces cerevisiae* harbouring xylose isomerase. BMC Biotechnol. 2014 May
607 15;14(1): doi:10.1186/1472-6750-14-41.
608 48. Bellissimi E, van Dijken JP, Pronk JT, van Maris AJA. Effects of acetic acid on the
609 kinetics of xylose fermentation by an engineered, xylose-isomerase-based
610 *Saccharomyces cerevisiae* strain. FEMS Yeast Res. 2009 May 1;9(3):358–64.
611 49. Ho CH, Magtanong L, Barker SL, Gresham D, Nishimura S, Natarajan P, et al. A
612 molecular barcoded yeast ORF library enables mode-of-action analysis of bioactive
613 compounds. Nat Biotechnol. 2009 Apr 6;27(4):369–77.
614 50. Sherman F. Getting started with yeast. Methods Enzymol. 2002 Jan 1;350:3–41.
615 51. Chundawat SPS, Vismeh R, Sharma LN, Humpula JF, da Costa Sousa L, Chambliss CK,
616 et al. Multifaceted characterization of cell wall decomposition products formed during

ammonia fiber expansion (AFEX) and dilute acid based pretreatments. Bioresour Technol. 2010 Nov 1;101(21):8429–38.

52. Sardi M, Rovinskiy N, Zhang Y, Gasch AP. Leveraging Genetic-background effects in *Saccharomyces cerevisiae* to improve lignocellulosic hydrolysate tolerance. Appl Environ Microbiol. 2016 Oct 1;82(19):5838–49.

53. Balan V, Bals B, Chundawat SPS, Marshall D, Dale BE. Lignocellulosic biomass pretreatment using AFEX. In: Mielenz J, editor. Biofuels. Methods in Molecular Biology (Methods and Protocols). Totowa, NJ: Humana Press; 2009. pp. 61–77.

54. Wenger CD, Phanstiel DH, Lee MV, Bailey DJ, Coon JJ. COMPASS: A suite of pre- and post-search proteomics software tools for OMSSA. Proteomics. 2011 Mar 1;11(6):1064–74.

55. Geer LY, Markey SP, Kowalak JA, Wagner L, Xu M, Maynard DM, et al. Open mass spectrometry search algorithm. J Proteome Res. 2004;3: 958–964. doi:10.1021/pr0499491.

56. Merrill AE, Hebert AS, MacGilvray ME, Rose CM, Bailey DJ, Bradley JC, et al. NeuCode labels for relative protein quantification. Mol Cell Proteomics. 2014 Sep 17;13(9):2503–12.

57. Thevelein JM, de Winde JH. Novel sensing mechanisms and targets for the cAMP-protein kinase A pathway in the yeast *Saccharomyces cerevisiae*. Mol Microbiol. 1999 Sep 1;33(5):904–18.

58. Neuman-Silberberg FS, Bhattacharya S, Broach JR. Nutrient availability and the RAS/cyclic AMP pathway both induce expression of ribosomal protein genes in *Saccharomyces cerevisiae* but by different mechanisms. Mol Cell Biol. 1995 Jun 1;15(6):3187–96.

59. Klein C, Struhl K. Protein kinase A mediates growth-regulated expression of yeast ribosomal protein genes by modulating *RAP1* transcriptional activity. Mol Cell Biol. 1994

643 Mar 1;14(3):1920–8.

644 60. Rittenhouse J, Moberly L, Marcus F. Phosphorylation in vivo of yeast (*Saccharomyces*
645 *cerevisiae*) fructose-1,6-bisphosphatase at the cyclic AMP-dependent site. J Biol Chem.
646 1987 Jul 25;262(21):10114–9.

647 61. Portela P, Howell S, Moreno S, Rossi S. In vivo and in vitro phosphorylation of two
648 isoforms of yeast pyruvate kinase by protein kinase A. J Biol Chem. 2002 Aug
649 23;277(34):30477–87.

650 62. Dihazi H, Kessler R, Eschrich K. Glucose-induced stimulation of the Ras-cAMP pathway
651 in yeast leads to multiple phosphorylations and activation of 6-phosphofructo-2-kinase.
652 Biochemistry. 2003;42(20): 6275-6282.

653 63. François J, Parrou JL. Reserve carbohydrates metabolism in the yeast *Saccharomyces*
654 *cerevisiae*. FEMS Microbiol Rev. 2001 Jan 1;25(1):125–45.

655 64. Enjalbert B, Parrou JL, Teste MA, François J. Combinatorial control by the protein
656 kinases PKA, PHO85 and SNF1 of transcriptional induction of the *Saccharomyces*
657 *cerevisiae GSY2* gene at the diauxic shift. Mol Genet Genomics. 2004 Jul 22;271(6):697–
658 708.

659 65. Hirimburegama K, Durnez P, Keleman J, Oris E, Vergauwen R, Mergelsberg H, et al.
660 Nutrient-induced activation of trehalase in nutrient-starved cells of the yeast
661 *Saccharomyces cerevisiae*: cAMP is not involved as second messenger. J Gen Microbiol.
662 1992 Oct 1;138(10):2035–43.

663 66. Durnez P, Pernambuco MB, Oris E, Argüelles J-C, Mergelsberg H, Thevelein JM.
664 Activation of trehalase during growth induction by nitrogen sources in the yeast
665 *Saccharomyces cerevisiae* depends on the free catalytic subunits of camp-dependent
666 protein kinase, but not on functional ras proteins. Yeast. 1994 Aug 1;10(8):1049–64.

667 67. Schepers W, Van Zeebroeck G, Pinkse M, Verhaert P, Thevelein JM. In vivo
668 phosphorylation of Ser21 and Ser83 during nutrient-induced activation of the yeast

protein kinase A (PKA) target trehalase. J Biol Chem. 2012 Dec 28;287(53):44130–42.

68. Ewald JC, Kuehne A, Zamboni N, Skotheim JM. The yeast cyclin-dependent kinase routes carbon fluxes to fuel cell cycle progression. Mol Cell. 2016 May 19;62(4):532–45.

69. Vallejo MC, Mayinger P. Delayed turnover of unphosphorylated Ssk1 during carbon stress activates the yeast Hog1 MAP kinase pathway. PLoS One. 2015 Sep 4;10(9): doi:10.1371/journal.pone.0137199.

70. Dihazi H, Kessler R, Eschrich K. High osmolarity glycerol (HOG) pathway-induced phosphorylation and activation of 6-phosphofructo-2-kinase are essential for glycerol accumulation and yeast cell proliferation under hyperosmotic stress. J Biol Chem. 2004 Jun 4;279(23):23961–8.

71. MacGilvray ME, Shishkova E, Chasman D, Place M, Gitter A, Coon JJ, et al. Network inference reveals novel connections in pathways regulating growth and defense in the yeast salt response. PLOS Comput Biol. 2018 May 8;13(5): doi:10.1371/journal.pcbi.1006088.

72. Albertyn J, Hohmann S, Thevelein JM, Prior BA. *GPD1*, which encodes glycerol-3-phosphate dehydrogenase, is essential for growth under osmotic stress in *Saccharomyces cerevisiae*, and its expression is regulated by the high-osmolarity glycerol response pathway. Mol Cell Biol. 1994 Jun 1;14(6):4135–44.

73. Brewster JL, Gustin MC. Positioning of cell growth and division after osmotic stress requires a map kinase pathway. Yeast. 1994 Apr 1;10(4):425–39.

74. Capaldi AP, Kaplan T, Liu Y, Habib N, Regev A, Friedman N, et al. Structure and function of a transcriptional network activated by the MAPK Hog1. Nat Genet. 2008 Nov 19;40(11):1300–6.

75. Kühn C, Petelenz E, Nordlander B, Schaber J, Hohmann S, Klipp E. Exploring the impact of osmoadaptation on glycolysis using time-varying response-coefficients. Genome Inform. 2008;20: 77-90.

76. Petelenz-Kurdziel E, Kuehn C, Nordlander B, Klein D, Hong K-K, Jacobson T, et al. Quantitative analysis of glycerol accumulation, glycolysis and growth under hyper osmotic stress. PLoS Comput Biol. 2013 Jun 6;9(6): doi:10.1371/journal.pcbi.1003084.

77. Babazadeh R, Furukawa T, Hohmann S, Furukawa K. Rewiring yeast osmostress signalling through the MAPK network reveals essential and non-essential roles of Hog1 in osmoadaptation. Sci Rep. 2015 May 15;4(1):4697.

78. Pisithkul T, Jacobson TB, O'Brien TJ, Stevenson DM, Amador-Noguez D. Phenolic amides are potent inhibitors of *de novo* nucleotide biosynthesis. Appl Environ Microbiol. 2015 Sep 1;81(17):5761–72.

79. Jayakody LN, Turner TL, Yun EJ, Kong II, Liu J-J, Jin Y-S. Expression of Gre2p improves tolerance of engineered xylose-fermenting *Saccharomyces cerevisiae* to glycolaldehyde under xylose metabolism. Appl Microbiol Biotechnol. 2018 Sep 19;102(18):8121–33.

80. Pampulha ME, Loureiro-Dias MC. Activity of glycolytic enzymes of *Saccharomyces cerevisiae* in the presence of acetic acid. Appl Microbiol Biotechnol. 1990 Dec;34(3):375–80.

81. Zhang G-C, Kong II, Wei N, Peng D, Turner TL, Sung BH, et al. Optimization of an acetate reduction pathway for producing cellulosic ethanol by engineered yeast. Biotechnol Bioeng. 2016 Dec 1;113(12):2587–96.

82. Wei N, Quarterman J, Kim SR, Cate JHD, Jin Y-S. Enhanced biofuel production through coupled acetic acid and xylose consumption by engineered yeast. Nat Commun. 2013 Dec 8;4(1): 2587-2596.

83. Colombo S, Ronchetti D, Thevelein JM, Winderickx J, Martegani E. Activation state of the Ras2 protein and glucose-induced signaling in *Saccharomyces cerevisiae*. J Biol Chem. 2004 Nov 5;279(45):46715–22.

84. Vandamme J, Castermans D, Thevelein JM. Molecular mechanisms of feedback inhibition of protein kinase A on intracellular cAMP accumulation. Cell Signal. 2012 Aug

1;24(8):1610–8.

85. Peeters T, Louwet W, Geladé R, Nauwelaers D, Thevelein JM, Versele M. Kelch-repeat proteins interacting with the Galpha protein Gpa2 bypass adenylate cyclase for direct regulation of protein kinase A in yeast. Proc Natl Acad Sci. 2006 Aug 29;103(35):13034–9.

86. Werner-Washburne M, Brown D, Braun E. Bcy1, the regulatory subunit of cAMP-dependent protein kinase in yeast, is differentially modified in response to the physiological status of the cell. J Biol Chem. 1991 Oct 15;266(29):19704–9.

87. Griffioen G, Anghileri P, Imre E, Baroni MD, Ruis H. Nutritional control of nucleocytoplasmic localization of cAMP-dependent protein kinase catalytic and regulatory subunits in *Saccharomyces cerevisiae*. J Biol Chem. 2000 Jan 14;275(2):1449–56.

88. Griffioen G, Branduardi P, Ballarini A, Anghileri P, Norbeck J, Baroni MD, et al. Nucleocytoplasmic distribution of budding yeast protein kinase A regulatory subunit Bcy1 requires Zds1 and is regulated by Yak1-dependent phosphorylation of its targeting domain. Mol Cell Biol. 2001 Jan 15;21(2):511–23.

89. Griffioen G, Swinnen S, Thevelein JM. Feedback inhibition on cell wall integrity signaling by Zds1 involves Gsk3 phosphorylation of a cAMP-dependent protein kinase regulatory subunit. J Biol Chem. 2003 Jun 27;278(26):23460–71.

90. Zhang A, Gao W. Mechanisms of protein kinase Sch9 regulating Bcy1 in *Saccharomyces cerevisiae*. FEMS Microbiol Lett. 2012 Jun 1;331(1):10–6.

91. Smith FD, Esseltine JL, Nygren PJ, Veesler D, Byrne DP, Vonderach M, et al. Local protein kinase A action proceeds through intact holoenzymes. Science. 2017 Jun 23;356(6344):1288–93.

92. Vigil D, Blumenthal DK, Brown S, Taylor SS, Trewhella J. Differential effects of substrate on type I and type II PKA holoenzyme dissociation. Biochemistry. 2004;43(19): 5629-5636.

747 93. Myers KS, Riley NM, MacGilvray ME, Sato TK, McGee M, Heilberger J, et al. Rewired
748 PKA signaling activates sugar and hypoxic responses for anaerobic xylose fermentation
749 in yeast. Under review at PLoS Genetics.

Supplementary Figure Legends

Supplementary Figure 1. 9% Growth and metabolism profiles in 9% ACSH. Batch cultures were grown in 9% ACSH anaerobically for 92 hours. Data represent average and standard deviation from three biological replicates. **A.** OD_{600} measurements over time. Glucose (**B.**) and xylose (**C.**) concentration in the media over time.

Supplementary Figure 2. Growth and metabolism profiles in 6% ACSH. As described in Supplementary Figure 1 except for anaerobic 6% ACSH growth, measuring dry-cell weight (**A.**), and glucose (**B.**), xylose (**C.**), and ethanol (**D.**) media concentration over time.

Supplementary Figure 3. Growth and metabolism profiles in YPDX 6%/3%. As described in Supplementary Figure 1 except for anaerobic YPDX 6%/3% growth, measuring dry-cell weight (**A.**), and glucose (**B.**), xylose (**C.**), and ethanol (**D.**) media concentration over time.

Supplementary Figure 4. High starting cell titers increases xylose consumption in nutrient-rich medium, but not ACSH. Batch cultures were grown anaerobically for 96 hours in YPDX 6%/3% (**A.**) or 6% ACSH (**B.**). Cultures were started at an OD_{600} of 3. Data represent average and standard deviation of three biological replicates. Comparing Panel A to Figure 3C shows that the Y184 Bcy1-AiD strain ferments xylose when the culture is inoculated at a higher starting OD but not when inoculated at a lower cell density.

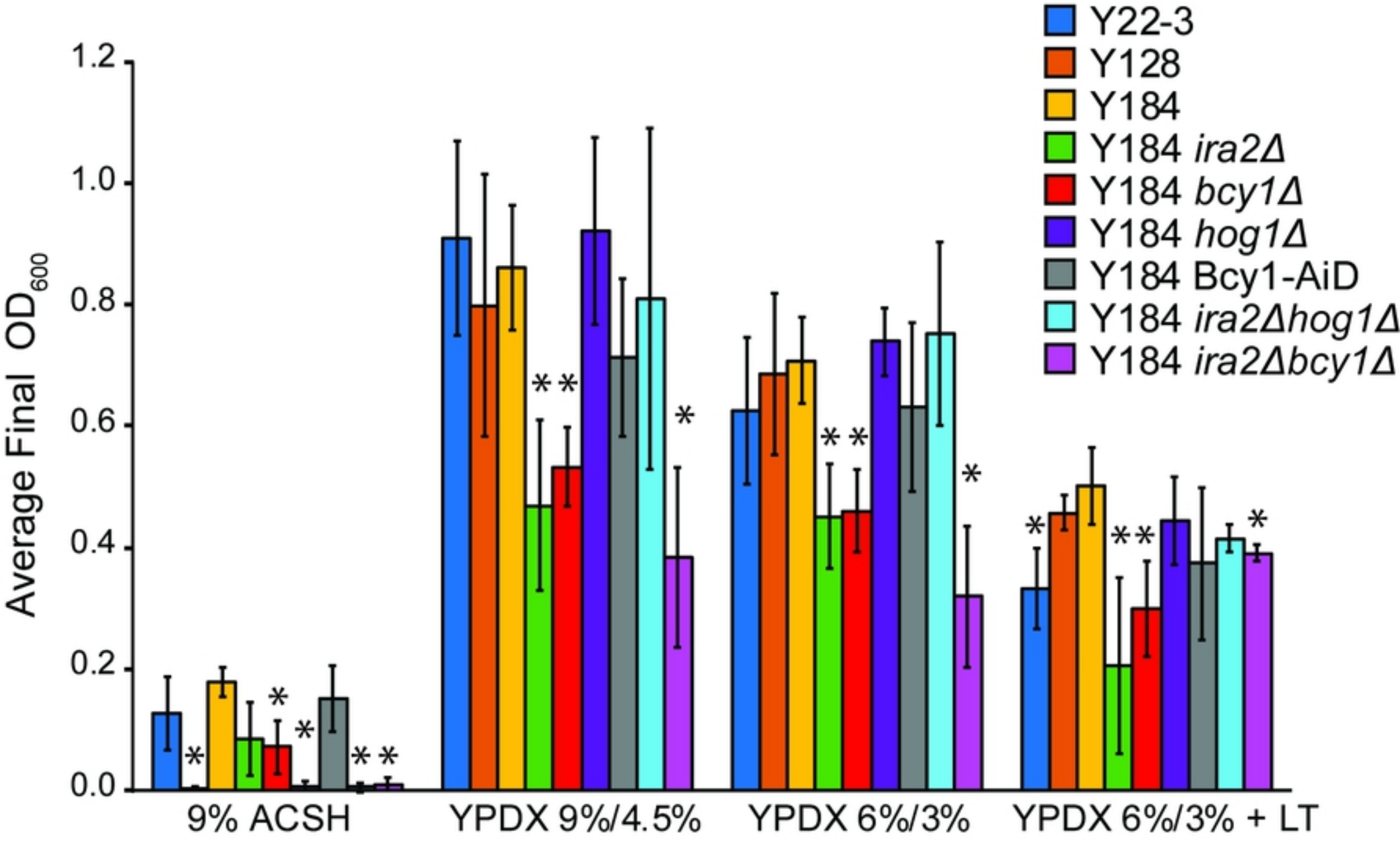
Y22-3
Y128
Y184
Y184 ira2Δ
Y184 bcy1Δ
Y184 hog1Δ
Y184 Bcy1-AiD
Y184 ira2Δhog1Δ
Y184 ira2Δbcy1Δ
Average Final OD600
1.2
1.0
0.8
0.6
0.4
0.2
0.0
9% ACSH
YPDX 9%/4.5%
YPDX 6%/3%
YPDX 6%/3% + LT

Figure 1

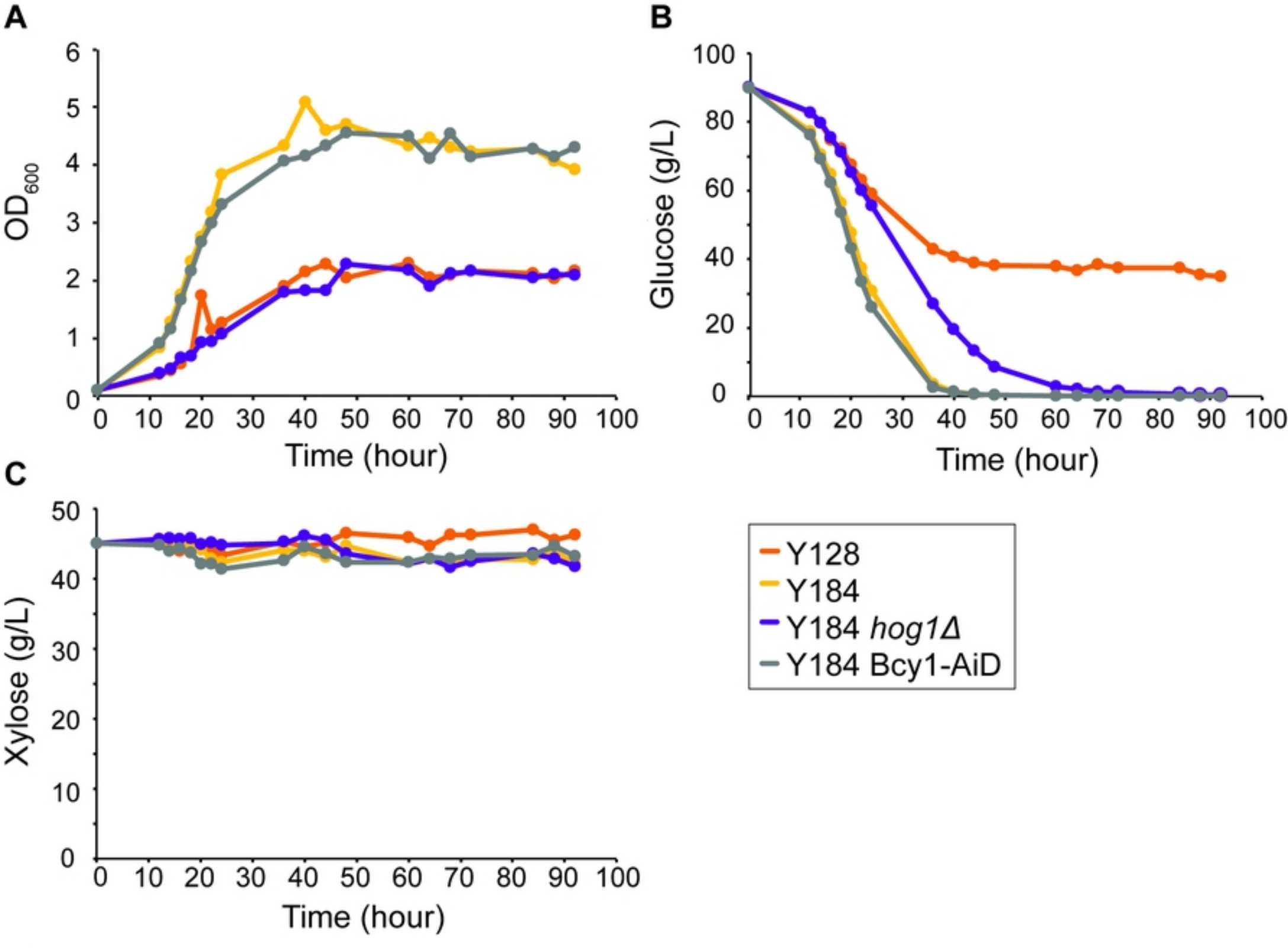
A
B
C
OD600
Time (hour)
Glucose (g/L)
Time (hour)
Xylose (g/L)
Time (hour)
Y128
Y184
Y184 hog1Δ
Y184 Bcy1-AiD

Figure 2

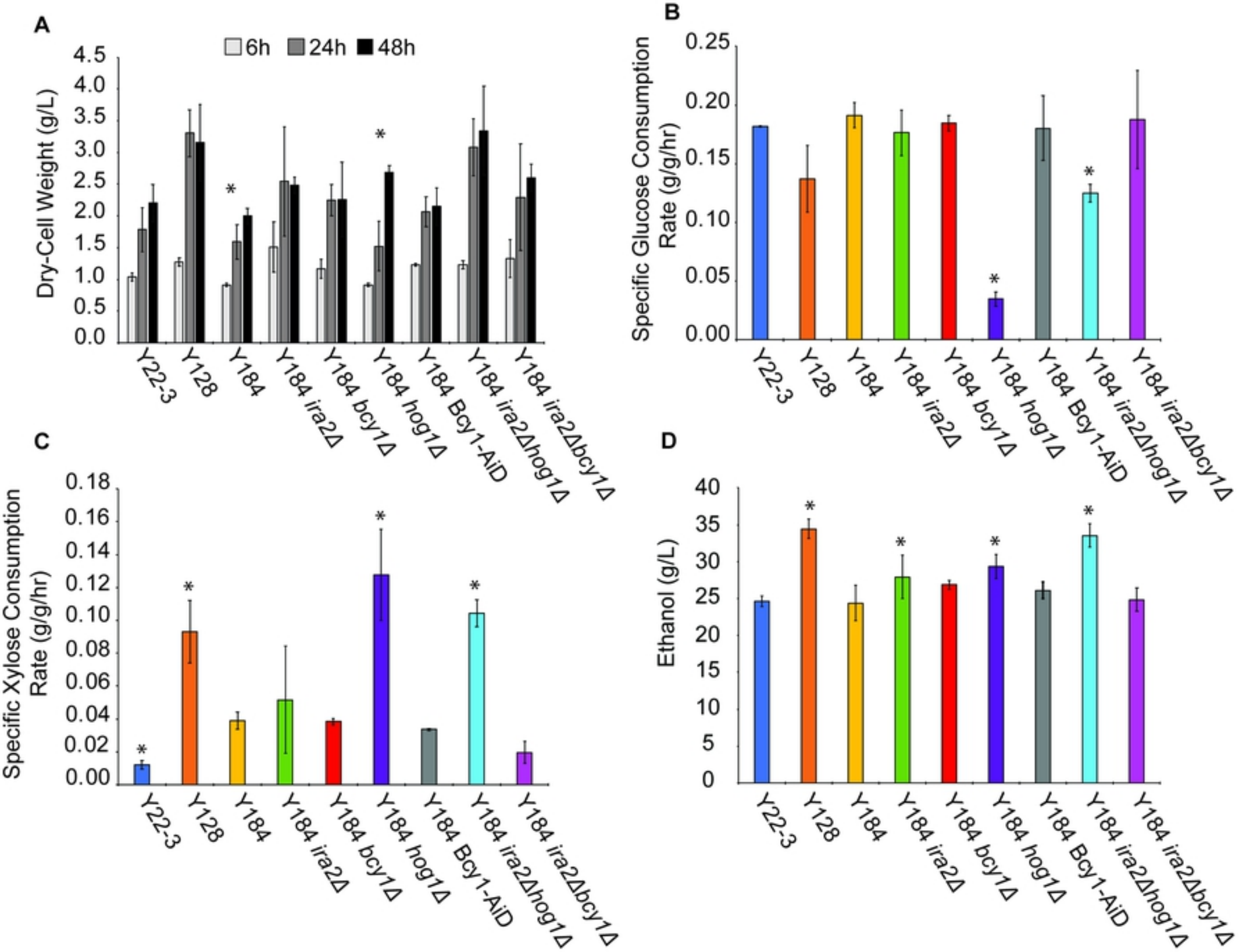
A
6h
24h
48h
Dry-Cell Weight (g/L)
4.5
4.0
3.5
3.0
2.5
2.0
1.5
1.0
0.5
0.0
*
*
Y22-3
Y128
Y184
Y184 ira2Δ
Y184 bcy1Δ
Y184 hog1Δ
Y184 Bcy1-AiD
Y184 ira2Δhog1Δ
Y184 ira2Δbcy1Δ
B
Specific Glucose Consumption Rate (g/g/hr)
0.25
0.20
0.15
0.10
0.05
0.00
*
*
Y22-3
Y128
Y184
Y184 ira2Δ
Y184 bcy1Δ
Y184 hog1Δ
Y184 Bcy1-AiD
Y184 ira2Δhog1Δ
Y184 ira2Δbcy1Δ
C
Specific Xylose Consumption Rate (g/g/hr)
0.18
0.16
0.14
0.12
0.10
0.08
0.06
0.04
0.02
0.00
*
*
*
Y22-3
Y128
Y184
Y184 ira2Δ
Y184 bcy1Δ
Y184 hog1Δ
Y184 Bcy1-AiD
Y184 ira2Δhog1Δ
Y184 ira2Δbcy1Δ
D
Ethanol (g/L)
40
35
30
25
20
15
10
5
0
*
*
*
Y22-3
Y128
Y184
Y184 ira2Δ
Y184 bcy1Δ
Y184 hog1Δ
Y184 Bcy1-AiD
Y184 ira2Δhog1Δ
Y184 ira2Δbcy1Δ

Figure 3

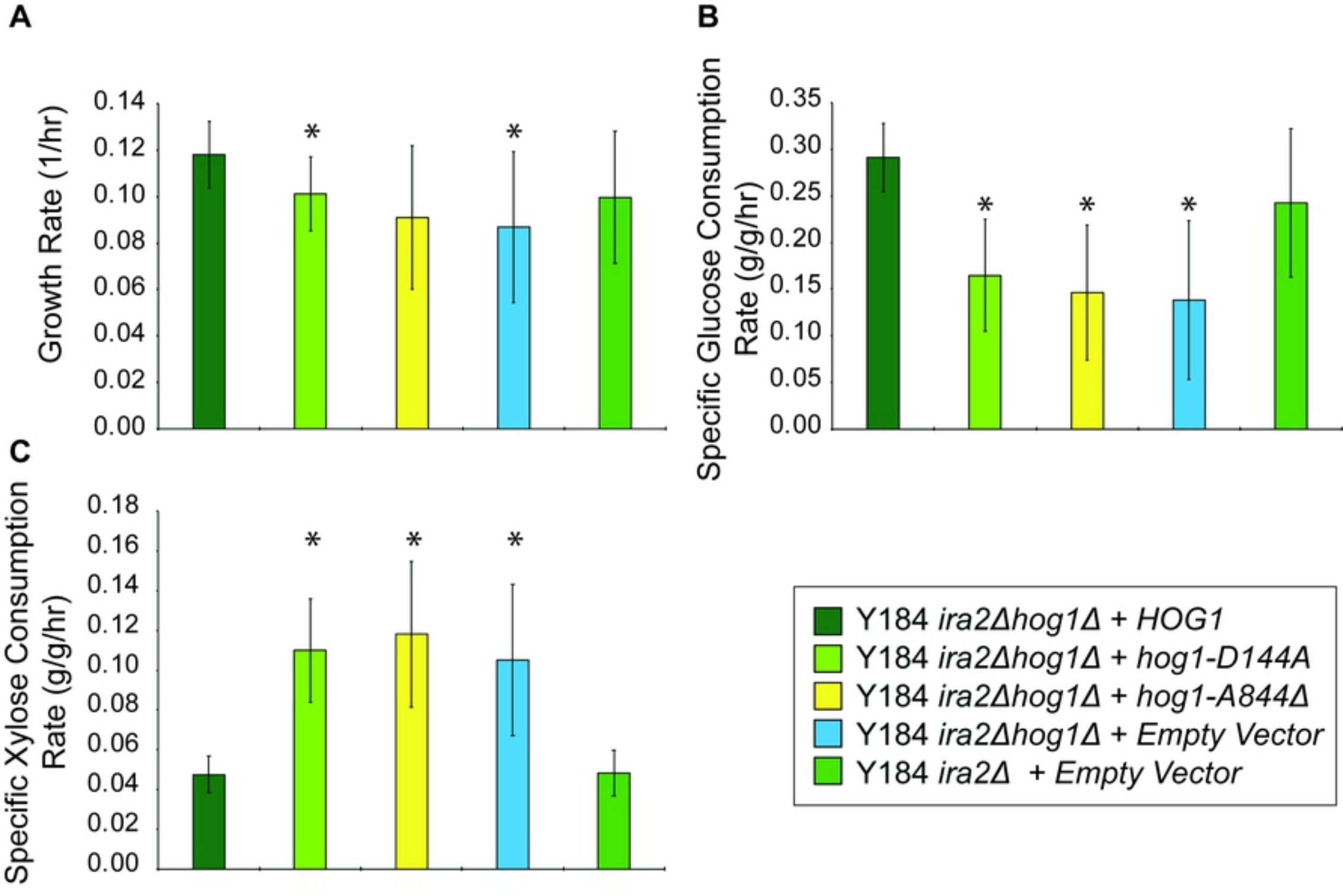
A
Growth Rate (1/hr)
0.14
0.12
0.10
0.08
0.06
0.04
0.02
0.00
*
*
B
Specific Glucose Consumption Rate (g/g/hr)
0.35
0.30
0.25
0.20
0.15
0.10
0.05
0.00
*
*
*
C
Specific Xylose Consumption Rate (g/g/hr)
0.18
0.16
0.14
0.12
0.10
0.08
0.06
0.04
0.02
0.00
*
*
*
Y184 ira2Δhog1Δ + HOG1
Y184 ira2Δhog1Δ + hog1-D144A
Y184 ira2Δhog1Δ + hog1-A844Δ
Y184 ira2Δhog1Δ + Empty Vector
Y184 ira2Δ + Empty Vector

Figure 4